ELSEVIER

Nuclear Physics B (Proc. Suppl.) 70 (1999) 74–78

NUCLEAR PHYSICS B
PROCEEDINGS
SUPPLEMENTS

# Current limits on the cold dark matter interaction cross section obtained by the UK collaboration

T. J. Sumner[a], J. J. Quenby[a], A. Bewick[a], N. J. T. Smith[a], W. G. Jones[a], T. Ali[a], B. Ahmed[a], D. Davidge[a], G. J. Davies[a], A. Howard[a], M. K. Joshi[a],* P. F. Smith[b], G. J. Homer[b], G. T. J. Arnison[b], J. D. Lewin[b], G. J. Alner[b], N. J. Spooner[c], L. Thompson[c], P. Sellin[c], S. Walker[c], J. Roberts[c], C. Peak[c] and J. C. Barton[d]

[a]Blackett Laboratory, ICSTM, London, SW7 2BZ, UK

[b]Particle Physics Department, RAL, Chilton, Didcot, Oxon, OX11 0QX, UK

[c]Department of Physics, University of Sheffield, Sheffield, S3 7RH, UK

[d]Department of Physics, Birkbeck College, London WC1E 7HX, UK

The UK Dark Matter Collaboration has run a 5-6 kg NaI detector in a well-shielded underground enviroment for about a year. Signatures of Cold Dark Matter (CDM) interactions are sought using pulse shape discrimination techniques by searching for the relatively short scintillation pulses arising from nuclear recoils among the residual, longer, background events from residual radioactivity in the detector and its environment. Here we report on an improvement to the limits on the CDM cross section for spin dependent interactions using our latest data from a crystal with improved detection efficiency and taking into account recent improved estimates of the spin factor correction between the nucleus and nucleon-supersymmetric particle cross sections.

## 1. INTRODUCTION

While the Galactic dark matter probably contain some mixture of massive, failed stars and relativistic neutrinos, it is believed that the gravitational potential of the Galaxy is most likely dominated by massive supersymmetric particles of energy density 0.3 GeV $cm^{-3}$ behaving as a Maxwell Boltzmann distribution with a most probable velocity of ~230 km $s^{-1}$, but truncated at high velocities by escape. The Earth streams through this distribution with a mean velocity of 244 km $s^{-1}$, but subject to an annual modulation. The ground state, lightest supersymmetric particles (LSP), which according to accelerator studies must exceed 40 GeV in mass [1], scatter elastically from nuclei to yield energy losses in the keV range.

An accepted theoretical estimate of the scattering cross section, $\sigma$, of an LSP by a nucleus when the LSP is a photino is equation (1) [2], which is the axial coupling case;

$$\sigma_T(cm^2) \simeq \frac{2G_F^2}{\pi\hbar^4}\left(\frac{109GeVc^{-2}}{m_{\tilde{q}}}\right)^4 \mu^2 I_s \qquad (1)$$

for CDM mass $M_D$, target mass $M_T$, $r = 4M_D\ M_T/\ (M_T + M_D)^2$ and $\mu^2 = M_D\ M_T\ r/\ 4$ where $\mu$ is the reduced mass. $m_{\tilde{q}}$ is the mass of the assumed degenerate exchange squark and $G_F^2/8\pi\hbar^4 = 2.11 \times 10^{-3}$ if $\mu$ is in $GeV/c^2$ and the result is in picobarn. $I_s$ is basically the spin structure function of the nucleus applying at zero momentum transfer. In the more general situation of the LSP being a mixture of "ino's" and assuming a full shell model treatment, the specific computations of Ressel and Dean [3], yield values of $I_s = C_{WN}^2\lambda^2\ J(J+1)_{eff}$ where $\lambda^2\ J(J+1)_{eff}$ is the shell model factor depending on both the LSP composition in terms of photino, Higgsino, Bino and Zino particles and the expectation value

*We thank Cleveland Potash Ltd for allowing us to use the Boulby mine and their support facilities, H. Vine of ICSTM and D.A. White, A. Nichols and V.W. Edwards of RAL for technical support and PPARC for funding the experiment. STARLINK computing facilities at ICSTM (also funded by PPARC) are used for much of the data analysis.


PII S0920-5632(98)00391-0

of the nucleus proton and neutron group spin content. $C_{WN}$ is the square hadronic matrix element for the LSP-nucleon interaction. The other terms in equation (1) then must be modified, but this form will both indicate the order of magnitude of the predicted cross-section and the correction necessary to go from $\sigma_Z$ to $\sigma_P$, ie nucleus $Z$ to the proton. $C^2_{WN} \sim 0.1$ from EMC measurements or the NQM model and $m_q \leq 1000$, so we expect $\sigma_P$ values as low as $10^{-3}$pb. The $\lambda^2\ J(J+1)_{eff}$ values adopted here for Na, Ge and I are respectively 0.097, 0.1 and 0.119, the I value in particular giving 'improved' experimental results as it is considerably higher than previous approximate estimates.

## 2. EXPERIMENTAL RESULTS

Experimental limits on the actual dark matter interaction rate come from well shielded, underground ionisation detectors. Initially, semiconductor germanium detectors provided the best results [4], but recently NaI(Tl) crystal scintillators have yielded successively improved spin dependent upper limits [5–7]. We reported [5] previously the results of a 6 month run with a 6.2 kg NaI(Tl) crystal, shielded by a 6 m diameter and 6 m deep pure water tank located 1100 m underground at Boulby, N. Yorkshire. The crystal was encapsulated in pure Cu and viewed by in coincidence by two 78 mm phototubes through 30 cm tapered silica light guides. Great efforts were made to reduce the residual radioactivity of the apparatus. Individual output pulse shapes were recorded, as was the detector temperature. Dark matter nuclear recoil events are expected to be like neutron collisions and as the residual neutron activity is minimal at the experiment, it is possible to distinguish between $\beta$ and $\gamma$ radioactivity in the crystal and potential dark matter interaction events on the basis of the different pulse decay times from the two classes of events. Exploitation of this relatively small difference ($\sim$ 20% at low energies) allows a factor ten gain in sensitivity. Calibration runs in the water shield with a Californium source emitting gammas and neutrons and a $^{57}$Co source just emitting gammas allowed pulse rise time distributions for neutrons and gammas separately to be determined. All rise times are found by a maximum likelihood, exponential fit.

Since our last published result deterioration in the crystal surface has required the crystal to be re-encapsulated with a reduction in mass to 5 kg. We have run this mass with 125 mm phototubes, viewed by cylindrical 18 cm long silica light guides. Figure 1 shows 78 days worth of new data, together with the 173 days previously obtained. Strict temperature control at $11° \pm 0.5°$ was obtained in the current run. The figure shows a count rate versus energy loss curve in events /kg/day/keV. The photoelectron yield was previously 1.72/keV and is now 3.1/keV; corrections have already been applied for Poisson statistics of photoelectron generation and the probability of triggering both phototube channels. Next, pulse decay time distributions are collected as a function of decay time and, for the first run these are corrected for a secular reduction in light collection efficiency, determined from regular source calibration runs and amounting to 2.5% / month. A further empirical decay time temperature coefficient of 5 nanosec/° K was also applied to this dataset. The recent data do not require significant temperature or drift correction. As shown earlier [6] the pulse height distributions in a particular energy band can be fitted by log gaussian differential distributions with a dimensionless width parameter $1.1 \leq w \leq 1.8$, so that the mean time constant, $\tau$ has a standard deviation $\sigma(\tau_d) = \tau_d\ ln(w)/N_f^{1/2}$ where $N_f$ is the number of events used to yield the distribution. This is the dominant error although some extra effects due to temperature correction and the statistics of the calibration are included in the previous run final error [5,6]. We measure in each run the differences as a function of scintillator energy loss between the calibration and underground background, $\Delta_{\gamma d} = (\tau_\gamma - \tau_d)$ and between gamma and neutron calibration, $\Delta_{\gamma n} = (\tau_\gamma - \tau_n)$. We find that the measured $\Delta_{\gamma d}$ lies within the $1.3\sigma(\tau_d)$ limits for 8 energy channels between 4 and 25 keV. Hence we use the measured background rates of figure 1, reduced in the ratio $1.3\sigma(\tau_d)/\Delta_{\gamma n}$ as a measure of the 90% confidence level dark matter interaction rate upper limit,

$dR/dE_v$. This is corrected to the total recoil energy loss $dR/dE_R = f_n(dR/dE_v)$ via the scintillator efficiency factor $f_n$.

## 3. DERIVATION OF THE CURRENT DARK MATTER CROSS SECTION LIMITS

To obtain the experimental limits to the dark matter cross sections, we use the methods described previously [6] where we first establish a reduced total event rate, $R_0$, in events /kg /day related to $\sigma_T$ by;

$$R_0 = \frac{377}{M_T M_D}\left(\frac{\sigma}{1pb}\right)\left(\frac{n_0 M_D}{0.3GeVcm^{-3}}\right) \times \left(\frac{v_0}{230\ km\ s^{-1}}\right) \quad (2)$$

where $v_0$ is the most probable dark matter velocity and $n_0$ is its number density. The cross section is corrected for finite nuclear size effects at finite recoil energy, $E_R$ in keV, by a form factor,

$$F_s^2(qR) = j_0(qR)^2,\ qR < 2.25, qR > 4.5 \quad (3)$$

$$F_s^2(qR) = constant = 0.047, 2.25 \leq qR \leq 4.5 \quad (4)$$

where the effective nuclear radius for atomic number A is $R \sim 1.1A^{1/3})$ fm, $j_0$ are Bessel function zeros and the momentum transfer q in units of $fm^{-1}$ is $q = (2M_T E_R)^{0.5})/\hbar$ where $(\hbar = 197.3MeVfm)$. Ressel and Dean [3] find this form adequate at the modest $q$ values involved here. Then observations are related to a differential event rate /kg/day/keV by;

$$dR/dE_R = (R_0/E_0 r)((\pi)^{0.5}/(4y)) \times [erf(x+y) - erf(x-y)]\,[F(E_R)]^2 \quad (5)$$

with $x = (E_R/E_0 r)^{0.5}$, $y = v_E/v_0$ and $E_0 = (1/2)M_D(v_0)^2$ where $v_E$ is the Earth's velocity relative to the Galaxy. The limits on $\sigma_T$ are calculated separately for the 8 eight energy channels and also separately for Na and I and are per kg of the individual elements. Comparison may be made with the Ge detector limits, assuming the interactions are spin dependent and hence relying on only the 8% of non-zero spin $^{73}Ge$ within the Ge detector. We correct to a proton related cross-section computing the RHS of the following equation,

$$\frac{\sigma_{Wp}}{\lambda^2 J(J+1)_{eff,p}}\left(\frac{C_{WN}}{C_{Wp}}\right)^2 = \sigma_T \times \frac{\mu_p^2}{\mu_T^2} \times \frac{1}{[\lambda^2 J(J+1)]_{eff,T}} \quad (6)$$

We combine separate values for each energy channel via

$$\hat{S} = 1/\sqrt{W}\ W_i = 1/S_i^2\ W = \sum_{i=1}^{N} W_i \quad (7)$$

for N estimates of 90% confidence level $S_i$. The results of the proton-related cross-section limit calculations are shown in figure 2 for our combined runs for Na and I separately and combined together and also for the germanium data [4]. Our numbers agree well with those of Bottino et al. [8], who have performed a similar analysis on our data, and our experimental limits are within $20 - -30\%$ of those of Bernabei et al. [7]. Compared with previous analysis, the new Iodine nuclear spin factor has resulted in better limits above 100 GeV. However, to perform a satisfactory search of the parameter space allowed by current accelerator limits on the LSP composition and squark properties, a further two orders of magnitude sensitivity increase is required for spin dependent interactions. For the spin-independent case, NaI work has yet to improve dramatically on the Ge limits.

## 4. FUTURE IMPROVEMENTS TO OUR NaI SCINTILLATOR

The 5 kg detector is currently running continuously and we have some 180 days of new data being analysed. The higher photoelectron yield obtained since the crystal was re-encapsulated is allowing us to study the pulse shapes in more detail and to refine our pulse shape discrimination technique in the light of new information on pulse components. Ultimately we expect these new higher precision data will offer us a factor of 2 improvement in cross section limits.

Additional steps which are being taken to improve our experiment include investigating crystal purification techniques both to lower the intrinsic crystal radioactivity and to improve the

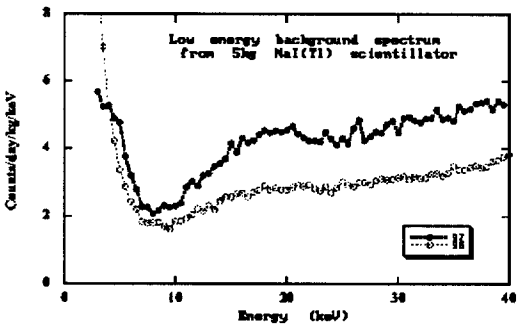


Figure 1. Background spectra; open circles are for data obtained in 1994 [5], closed circles are for data obtained in 1996/7.

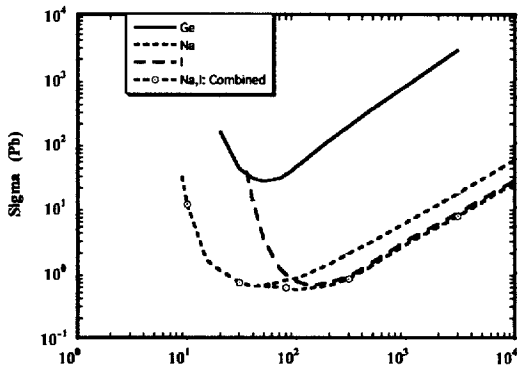


Figure 2. Dark matter cross section limits in picobarns, corrected to the equivalent proton cross section, as a function of LSP mass for the combined data of figure 1.

light output, and the development of large area avalanche photodiodes (APDs) to replace the intrinsically radioactive ($10^5\,\gamma$/day) photomultipliers [9]. The improved light collection, from removing the light guides, together with an improved quantum efficiency will increase the photoelectron yield to at least 20 photoelectron/keV and provide an immediate factor of 3 improvement in the potential nuclear recoil discrimination. In addition APDs are best suited to the 'UVIS' type detector [10] working at lower temperatures with undoped crystals. The detector geometry would need to be in the form of a segmented array with each element being viewed by one of two large area (~few $cm^2$) APDs. Such a geometry would also allow for mutual veto discrimination between elements.

Between them the various enhancements described should allow us to realise an order of magnitude lowering of the limits from the NaI scintillator experiments.

## 5. DEVELOPMENT OF A LIQUID XENON EXPERIMENT

In order to extend our sensitivity into the deeper reaches of the allowed LSP parameter space we believe it is necessary to achieve better background rejection than is possible with the NaI experiments. A first stage pilot experiment which uses liquid xenon as a scintillator to which pulse shape discrimination is applied is already funded and being built (see figures 3 & 4).

A second stage using additional ionisation and proportional signal channels will follow with the promise of reaching two orders of magnitude sensitivity below that of the NaI experiments [11]. We anticipate APDs will also be deployed for photon readout in this experiment.

## REFERENCES

1. J. Ellis et al., CERN-TH/97-105 UMN-TH-1537/97 TPI-MINN-97/16.
2. J.D. Lewin and P. F. Smith, Astr. Part. Phys. 6 (1996) 87.
3. M.T. Ressel and D.J. Dean, The Identifica-

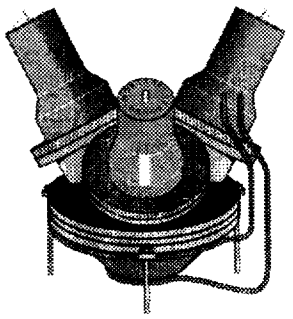

Figure 3. First stage liquid xenon scintillation detector.

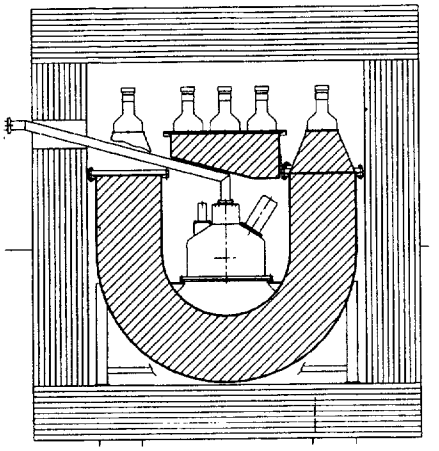

Figure 4. First stage assembly for liquid xenon detector showing its incorporation into a surrounding liquid scintillator veto shield.

tion of Dark Matter, World Scientific, Singapore, 1997, 318.
4. D.O. Caldwell et al., Phys. Rev. Lett. 61 (1988) 510.
5. J.J. Quenby et al., Astr. Part. Phys. 5 (1996) 249.
6. P.F. Smith et al., Phys. Letts. B 379 (1996) 299.
7. R. Bernabei et al., Phys. Letts. B389 (1996) 757.
8. A. Bottino et al., Phys. Letts. B402 (1997) 113.
9. T.J. Sumner and T. Ali, in The Identification of Dark Matter, World Scientific, Singapore, 1997, 557.
10. N.J.C. Spooner and P.F. Smith, Phys. Letts. B 314 (1993) 430.
11. W.G. Jones et al., in The Identification of Dark Matter, World Scientific, Singapore, 1997, 428 i